ATLAS luminosity determination in 2010

M. Huhtinen *CERN, CH-1211 Geneva, Switzerland*
on behalf of the ATLAS Luminosity WG

Abstract

This paper describes the detectors and algorithms which were used for monitoring the ATLAS luminosity in 2010. A main emphasis is on the absolute calibration by van der Meer scans. The systematic uncertainties associated with the calibration are discussed. The resulting uncertainty of the luminosity calibration reached in 2010 is 3.4%.

INTRODUCTION

The absolute luminosity of a particle collider can be written as

$$\mathcal{L} = \frac{R n_b f_r}{\sigma} \tag{1}$$

where n_b is the number of colliding bunches, f_r the revolution frequency, R the average rate of some process and σ the cross-section corresponding to that process.

Eq. 1 implies that any process that can be observed by the detector and for which the cross-section is known can be used to monitor luminosity. In the ideal case the dependence between the true rate (R) and the observed rate (εR) would be linear, but any well understood functional dependence is acceptable.

In ATLAS [1] the online luminosity measurement is based on detectors in the forward hemisphere, which record inelastic pp-collisions with an *a priori* unknown efficiency (ε). For the initial LHC start-up these efficiencies were estimated from Monte-Carlo simulations, and thus were associated with significant uncertainties – estimated to be at the level of 20% [2]. The purpose of an absolute luminosity calibration is to determine these efficiencies as accurately as possible. Provided the efficiencies remain stable in time and their dependence on pile-up can be accurately modelled the calibrated detector will yield an absolute luminosity measurement.

The average number of inelastic collisions per bunch-crossing, μ, follows a Poisson-distribution. We derive a quantity $\mu_{\mathrm{vis}} = \varepsilon\mu$ and correspondingly a visible cross-section

$$\sigma_{\mathrm{vis}} = \varepsilon\sigma_{\mathrm{inel}}, \tag{2}$$

both of which are detector-dependent. These allow to rewrite Eq. 1 as

$$\mathcal{L} = \frac{\mu n_b f_r}{\sigma_{\mathrm{inel}}} = \frac{\mu_{\mathrm{vis}} n_b f_r}{\sigma_{\mathrm{vis}}}, \tag{3}$$

where the luminosity depends only on a "fill constant" $n_b f_r$, the observed μ_{vis} and the calibration constant σ_{vis}.

LUMINOSITY MONITORING IN ATLAS

During the 2010 pp-running several luminosity detectors and algorithms, listed in Table 1, were used in ATLAS. These can be divided into "online" and "offline" methods. While the offline methods allow for more detailed analysis like timing cuts to identify collisions, their drawback in general is that they can only work from recorded events and thus have to deal with significantly lower statistics. Also, they are not available for fast online monitoring, e.g. when optimising the collisions by mini-scans. Online methods use the detector data-stream directly – in the case of MBTS the trigger rates before prescale – and thus have maximum statistics at their disposal. Only the online methods are able to provide luminosity information to the ATLAS control room (ACR) and to the LHC.

Some of the online methods can be applied at a frequency of order 1 Hz. This results in the instantaneous values displayed in the ACR and transmitted to LHC.

In normal stable-beam running of the LHC it can be assumed that the luminosity is essentially stable on the timescale of minutes. Therefore each ATLAS run is subdivided into luminosity blocks (LB) with a typical length of 2 minutes. This is the smallest quantity in which luminosity can be accounted in an offline analysis. The luminosities from all online methods are stored per LB in the COOL database.

One motivation to maintain several luminosity monitors and algorithms is to have fallback alternatives in case of problems with some detector. But an even more important aspect of this redundancy is to have a handle on systematic effects and long term stability. Inter-comparison of the detectors allows to diagnose potential drifts of efficiency in any given detector and enable us to investigate and fix potential problems promptly.

PILEUP DEPENDENCE OF ALGORITHMS

In 2010 only *Event counting* was used in ATLAS. This means counting the bunch-crossings where

- a signal is detected on either side of the detector (Event-OR)
- a signal is detected on both sides of the detector (Event-AND)

Event counting is related to *Zero counting* by

$$P_{\mathrm{Event}} = 1 - P_{\mathrm{Zero}}, \tag{4}$$

where P denotes the probability to observe an event (or zero, i.e. no event) in a given bunch crossing.

Table 1: Luminosity detectors and algorithms commissioned as luminosity detectors during the 2010 pp run. †The track counting algorithm is described in detail in [3].

Detector	Algorithms	per-bunch	Onl/Offl	Comments
LUCID	OR, AND	yes	Online	Provided preferred luminosity
MBTS	AND, (OR)	no	Online	Not usable with 150 ns bunch trains
BCM	OR, AND, XOR	yes	Online	Fully commissioned only end of September
MBTS timing	AND	yes	Offline	Coincidence within 10 ns
LAr timing	AND	yes	Offline	Used only in very early runs
Prim.Vtx	4 tracks	yes	Offline	p_T threshold for tracks 150 MeV/c
Track counting	≥ 1 track†	yes	Offline	Studied for comparisons between experiments

Denoting by $P_0(\mu)$ the probability to have no collision when the average number of Poisson-distributed collisions is μ, we obtain from Eq. 4 the probability $P_{\rm OR}(\mu)$ to have an "OR" event as

$$P_{\rm OR}(\mu) = 1 - P_0(\mu) = 1 - e^{-\mu}. \quad (5)$$

In Event-OR counting also $\mu_{\rm vis} = \varepsilon\mu$ follows a Poisson distribution and Eq. 5 is valid also if $\mu \to \mu_{\rm vis}$.

For Event-AND counting the situation is more complicated. The efficiency to observe a coincidence is given by $P_{\rm AND}(\mu) = P_{\rm A}(\mu) + P_{\rm C}(\mu) - P_{OR}(\mu)$, where A and C denote the two sides of the detector. The probability of a coincidence is then given as [4]

$$P_{\rm AND}(\mu) = 1 - e^{-\mu\varepsilon_{\rm A}} - e^{-\mu\varepsilon_{\rm C}} + e^{-\mu\varepsilon_{\rm OR}}. \quad (6)$$

If $\varepsilon_{\rm A} = \varepsilon_{\rm C}$, this can be simplified to

$$P_{\rm AND}(\mu) = 1 - 2e^{-\mu(\varepsilon_{\rm AND}+\varepsilon_{\rm OR})/2} + e^{-\mu\varepsilon_{\rm OR}}. \quad (7)$$

Using the definitions from Eq. 2 and $\mu_{\rm vis} = \varepsilon_{\rm AND}\mu$ allows to further rewrite this in the form

$$P_{\rm AND}(\mu_{\rm vis}) = 1-2e^{-\mu_{\rm vis}(1+\sigma_{\rm vis}^{\rm OR}/\sigma_{\rm vis}^{\rm AND})/2}+e^{-\mu_{\rm vis}\sigma_{\rm vis}^{\rm OR}/\sigma_{\rm vis}^{\rm AND}} \quad (8)$$

The luminosity determination is based on a measurement of $P(\mu)$ and while Eq. 5 is readily inverted, there is no analytical solution for Eq. 8. Except for approximate solutions for small μ or when $\sigma_{\rm vis}^{\rm OR} \approx \sigma_{\rm vis}^{\rm AND}$, the solution has to be found numerically.

In the special case of a van der Meer scan, when the $\sigma_{\rm vis}$ values are not yet known, the solution has to be found iteratively: first $\sigma_{\rm vis}^{\rm OR}$ is determined from a fit using the correction from Eq. 5 and then $\sigma_{\rm vis}^{\rm AND}$ from Eq. 8 by several iterative fits.

LUMINOSITY DETERMINATION FROM VAN DER MEER SCANS

The luminosity can also be calculated from beam parameters as

$$\mathcal{L} = \frac{n_b f_r n_1 n_2}{2\pi\Sigma_x\Sigma_y} \quad (9)$$

where n_1 and n_2 are the number of particles in the colliding bunches and Σ_x and Σ_y the convolved horizontal and vertical beam sizes.

By setting equal Eqs. 3 and 9 at the peak of the scan we obtain

$$\sigma_{\rm vis} = \frac{2\pi\mu_{\rm vis}^{\rm max}\Sigma_x\Sigma_y}{n_1 n_2} = 2\pi\mu_{\rm vis}^{\rm sp,max}\Sigma_x\Sigma_y, \quad (10)$$

which is the basic equation for the van der Meer (vdM) calibration [5]. The last step in Eq. 10 introduces the specific μ-value, $\mu_{\rm vis}^{\rm sp} = \mu/(n_1 n_2)$. Eq. 10 allows to obtain the calibration parameters $\sigma_{\rm vis}$ from measured scan data ($\mu_{\rm vis}^{\rm max}$, Σ_x and Σ_y) and a simultaneous determination of the bunch intensities. This provides the parameter $\sigma_{\rm vis}$ needed for the absolute calibration of the luminosity.

The values of Σ_x and Σ_y have to be determined in 2 scans along the corresponding axes. Inevitably these two scans are separated in time and due to emittance growth during the scan will result in slightly different $\mu^{\rm max}$-values. In Eq. 10 we use the arithmetic average of these two μ-values, i.e. the final formula for $\sigma_{\rm vis}$ is

$$\sigma_{\rm vis} = \pi(\mu_{\rm vis,x}^{\rm sp,max} + \mu_{\rm vis,y}^{\rm sp,max})\Sigma_x\Sigma_y. \quad (11)$$

The specific luminosity per bunch is obtained from Eq. 9 by dividing with the intensity product $n_1 n_2$ and the number of bunches:

$$\mathcal{L}_{\rm sp} = \frac{f_r}{2\pi\Sigma_x\Sigma_y} \quad (12)$$

It can be seen that, unlike $\sigma_{\rm vis}$, the value of $\mathcal{L}_{\rm sp}$ does not depend on any quantities that would involve properties of the detector or algorithm and therefore is an ideal quantity to study the consistency of different detectors and algorithms.

THE VDM SCANS

In 2010 ATLAS had 5 fills with vdM scans, of which one was dedicated to a length-scale calibration only and one was with heavy-ions. The first 3 fills listed in Table 2 had a total of 5 scan pairs. The very first scan in fill 1059 had a single scan in x and another in y. This was soon followed by a more extensive vdM session with first 2 scans in x, followed by 2 in y. Both of these were done with a single colliding bunch and very moderate μ.

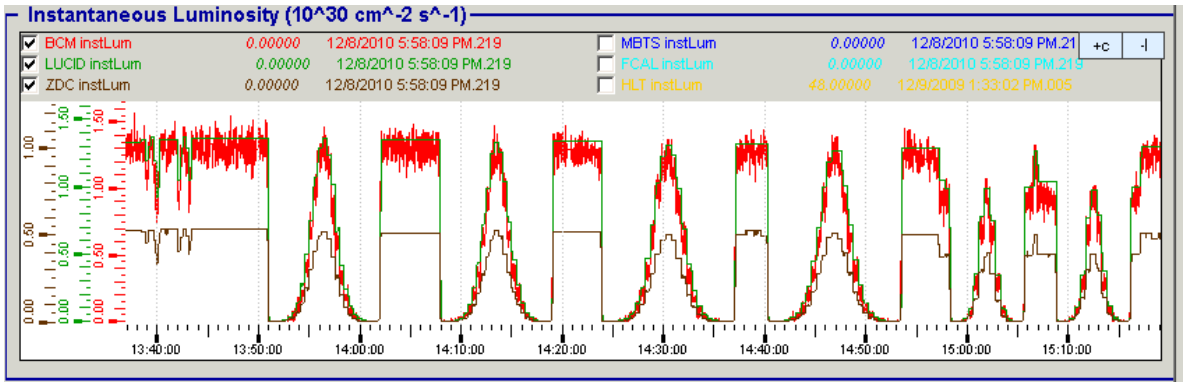

Figure 1: Illustration of the vdM scan procedure in ATLAS during LHC fill 1386. The first four scans are in order x, y, x, y with the other coordinate centred. The last two scans are in order x, y, with the other coordinate displaced by 60 μm. The time axis is in CEST.

Each of the october scans consisted of 25 points where luminosity data was recorded for 15–20 seconds. Between these acquisition points were shorter periods during which the beams were moved. During the scan luminosity recording by ATLAS LB's was disabled, instead a special scan-controller received information from the LHC and issued pseudo-LB boundaries accordingly.

The last vdM scans in October were done by alternating x and y scans. The time between 2 scans was about 20 minutes, i.e. all 4 scans fitted into a bit more than one hour. This procedure is illustrated in Fig. 1 as a function of real time. Scan-data stored in COOL per pseudo-LB was used for the vdM analysis.

The October fill also included 2 scans with a displacement in the other coordinate. This was intended to study xy-coupling, but the analysis of it has not yet finished. The centred scans, however, show no signs of significant coupling.

In all of the scans both beams were scanned simultaneously over $\pm 3\,\sigma_{\rm beam}$ in opposite directions giving a total maximum separation of $\pm 6\,\sigma_{\rm beam}$.

Fig. 2 shows the LUCID-EventOR luminosity as a function of BCID in fill 1386. Five of the colliding bunches are easily recognised, the sixth in BCID 1 is difficult to see in the Figure. Each colliding BCID is followed by a tail of "afterglow", which will be discussed later as a source of systematic uncertainty. On top of this tail sit the 26 non-colliding bunches.

FIT MODEL

Analysing the vdM scan data it was soon discovered that a single Gaussian does not provide a satisfactory fit. Since in most algorithms the background is negligible, adding a constant term did not bring significant improvement. A much better fit was obtained by a double-Gaussian with a constant background term:

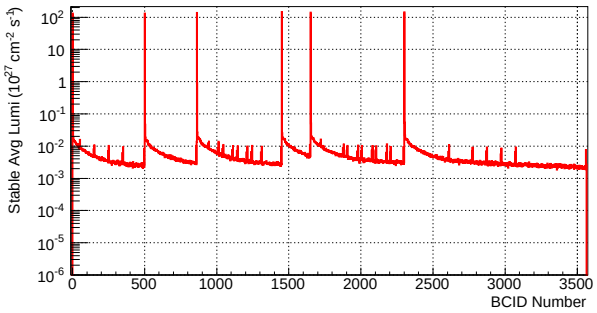

Figure 2: Luminosity as determined from LUCID-EventOR during LHC fill 1386. The large peaks correspond to the 6 colliding bunches while the 26 smaller peaks are due to the 13 unpaired bunches per beam. The slowly decaying tails are the "afterglow" discussed in the text

$$P(x) = \frac{P_0}{\sqrt{2\pi}}\left[\frac{f e^{-(x-x_0)^2/2\sigma_a^2}}{\sigma_a} + \frac{(1-f)e^{-(x-x_0)^2/2\sigma_b^2}}{\sigma_b}\right] + c \tag{13}$$

The convolved beam size can be obtained from these two Gaussians as

$$\frac{1}{\Sigma} = \left[\frac{f}{\sigma_a} + \frac{1-f}{\sigma_b}\right] \tag{14}$$

Setting $x = x_0$ in Eq. 13, we get

$$P(x_0) = \frac{P_0}{\sqrt{2\pi}}\left[\frac{f}{\sigma_a} + \frac{1-f}{\sigma_b}\right] = \frac{P_0}{\sqrt{2\pi}\Sigma} \tag{15}$$

If Eq. 14 is used to substitute, e.g., σ_b in Eq. 13 the resulting equation has Σ conveniently as its fit parameter.

A typical fit with Eq. 13 is shown in Fig. 3 together with the residuals.

Fig. 4 shows the distribution of χ^2/ndf for the fits on LUCID data, illustrating the good quality of the fits, which

Table 2: Summary of the vdM fills used by ATLAS in 2010

Date	Fill	Number of coll. bunches	β^* (m)	Crossing ang. (μrad)	N_b 10^{11}	μ at peak	Comment
Apr 26	1059	1	2	0	0.1	0.03	Scan 1 & length scale
May 9	1089	1	2	0	0.2	0.11	Scans 2 & 3
Oct 1	1386	6	3.5	200	0.9	1.4	Scans 4 & 5
Oct 4	1393	186	3.5	200	1.0	2.4	Length Scale
Nov 30	1533	113	2.5	0	0.1	0.00016	Heavy Ion

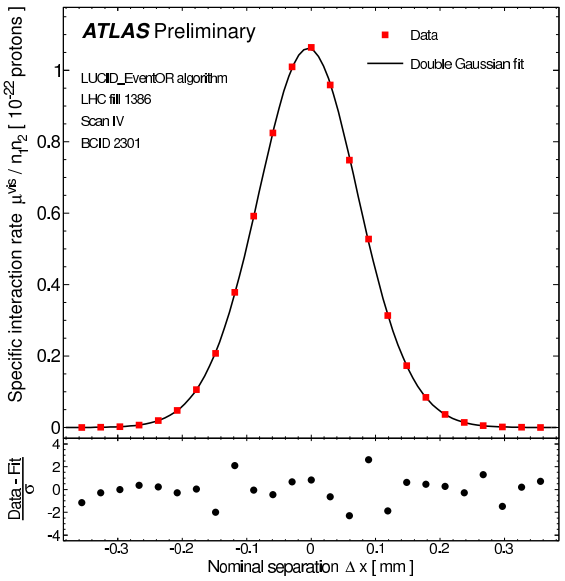

Figure 3: Fit of Eq. 13 to LUCID-EventOR data from scan IV in the x-plane. The residuals on the bottom plot are based on statistical deviations only [6].

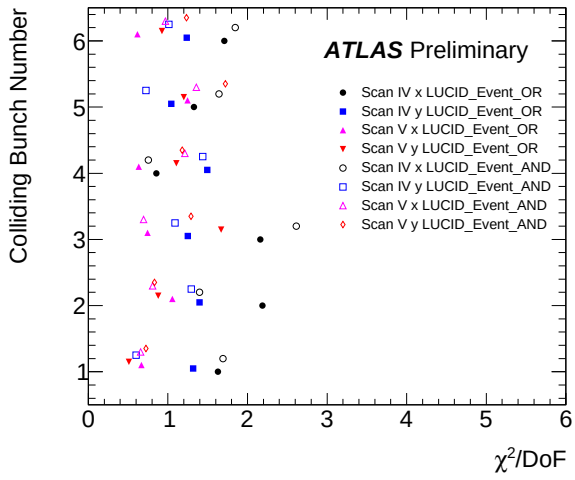

Figure 4: Distribution of $\chi^2/$ per number of degrees of freedom (ndf) values for fits to the LUCID vdM data.

suggests that a possible systematic error due to the fit function is small. Detailed studies using cubic spline fits and comparing the resulting $\sigma_{\rm vis}$ values allow to estimate the associated systematic effect as 0.2% for the october scans.

SYSTEMATIC UNCERTAINTIES

Bunch charge product

The uncertainty on the product n_1n_2 measured during the scan by LHC instrumentation has been significantly reduced by very detailed analysis [7], but with 3.1% remains to be the dominating uncertainty in the October scans.

Background and afterglow

The background due to beam-gas and beam-halo can be measured from the unpaired bunches shown in Fig. 2, but also from the tails of the fits to the scan data. Both methods indicate that this contribution is at the level of 10^{-4} for OR algorithms and negligible for the AND.

Afterglow refers to signals from the luminosity detectors after a colliding bunch pair. After each paired BCID we observe a long tail of signals up to the μs range, which we attribute to slow collision debris. In particular slow neutrons are susceptible to cause delayed signals via nuclear reactions which result in de-excitation by photon emission.

Emittance growth

During a fill the emittance of the beam grows, which results in a simultaneous increase of Σ and decrease of $\mu_{\rm vis}$. In principle these effects cancel each other, but in practice this cancellation is not exact since the values are determined over a longer time, i.e. Σ's result from fits to several data-points spread in time and for $\mu_{\rm vis}$ we use the average of 2 scans, roughly 20 minutes apart.

There are various methods to estimate the emittance growth:

1. From wire-scanner and synchrotron light monitor data recorded by the LHC

2. From the decrease of $\mu_{\rm vis}$ between the scans, when beams were colliding head-on

3. From the fits of Σ and $\mu_{\rm vis}$ to the scan curves

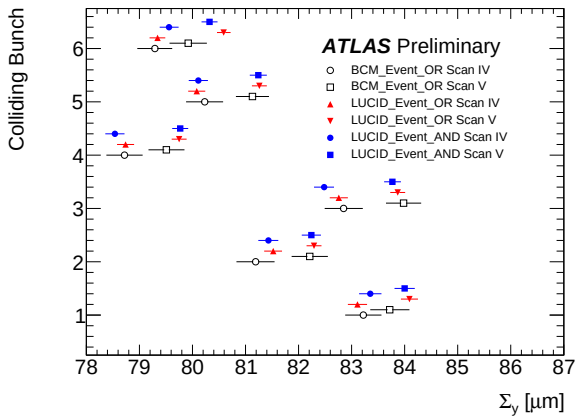

Figure 5: Σ_y for each colliding bunch pair, as determined from LUCID and BCM-EventOR data during the October scans. The error bars are statistical only and thus much larger for BCM which has a smaller count rate.

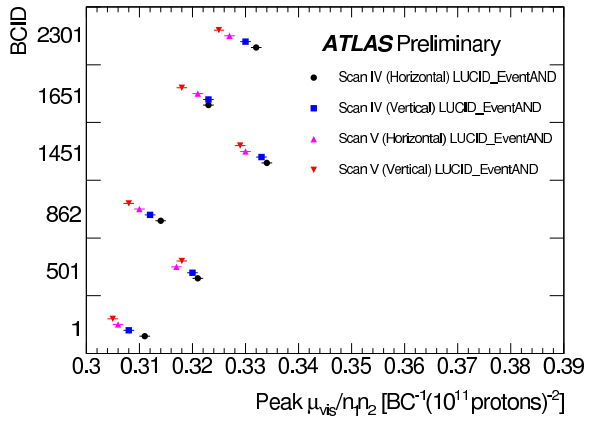

Figure 6: $\mu_{\rm vis}^{\rm sp,max}$ for each colliding bunch pair, as determined from LUCID-EventAND data. The error bars are statistical only.

The last of these can be seen in Figs. 5 and 6 and indicate an emittance increase of about 2% between scans IV and V. This is consistent with observation from the first 2 methods.

However, a comparison of the $\sigma_{\rm vis}$ values, obtained from the two scan-pairs, as shown in Fig. 7, confirms that the effect of emittance growth almost entirely cancels. The residual effect is $< 0.5\%$. It should be noted that this observed discrepancy between the scans accounts not only for the emittance growth but also for any other potential non-reproducibility effect.

Length scale

In Fig. 3 the luminosity data is plotted against the nominal beam separation, which is given by the currents in the separation magnets. In order to check this scale and dedicated length-scale calibration was done. The procedure was to displace one beam at the time and move the other until collisions were optimised at the offset position. At several such points data was taken and the ATLAS Inner Detector was used to reconstruct the primary vertex distribution. The correlation – an example is shown in Fig. 8 – between the shift of the reconstructed luminous centroid and the nominal displacement allowed to establish the length scale correction and uncertainty. The correlation was found to be excellent, so no correction was applied and an uncertainty of 0.3% was derived.

However, also an uncertainty related to the ID geometry enters. If the geometry of the ID would be distorted it could

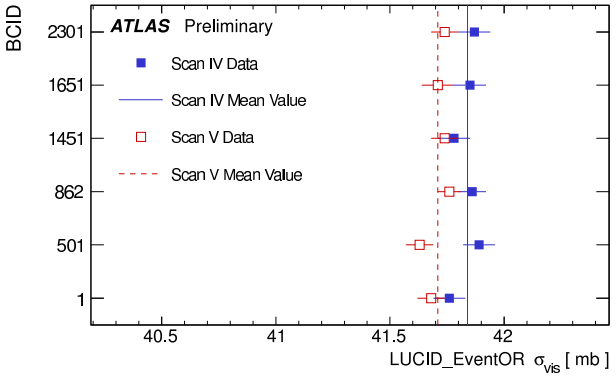

Figure 7: Values of $\sigma_{\rm vis}$ for each colliding bunch pair, as determined from LUCID-EventOR data. The error bars are statistical only.

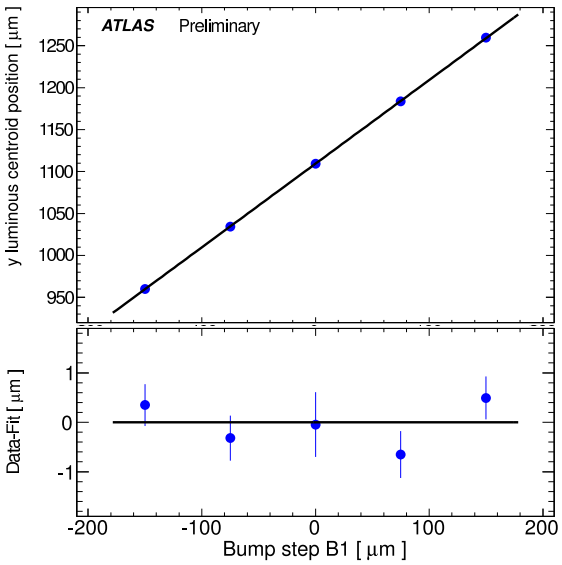

Figure 8: Length-scale calibration scan for the y direction of beam 1. The top plot shows the displacement of the luminous region as a function of the nominal displacement. The lower plot shows the residuals with respect to the linear fit.

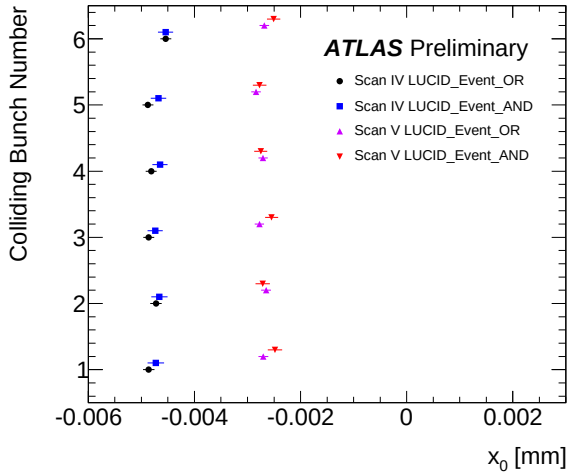

Figure 9: Values of x-displacement obtained from scans IV and V. After scan IV the displacement observed in online monitoring was corrected for. Nevertheless, a slightly smaller shift appeared in scan V.

lead to a wrong reconstructed displacement. These effects were studied by Monte Carlo using the extreme limit of data-driven alignment. These studies allowed to assign a conservative 0.3% uncertainty on the luminosity calibration due to this effect.

Beam centring and jitter

A potential source of error for the vdM scan is if the beams are not properly centred in one coordinate while the other is scanned. Our procedure of interleaved x and y scans allows to estimate the possible displacement and to correct for it if needed. In the October scans we observed perfect stability of the y-coordinate. However, Fig. 9 shows that there was indeed drift in x at the level of few μm. Compared to the beam-sizes during the scan this displacement corresponds to an uncertainty of only 0.04%.

Another source of uncertainty is a possible jitter of the beam position around its nominal value. A jitter of 0.8 μm measured during the length-scale calibration scan translates into an uncertainty of 0.3% on $\sigma_{\rm vis}$ [6]

Transverse correlations

Non-linear transverse correlations were discovered in the final stages of the analysis as a potentially important uncertainty. However, a detailed analysis allowed to estimate their effect to be only 0.9% in the October scans [6].

Summary of systematic effects

The evaluation of all components of the systematic uncertainty are discussed in detail in Ref. [6]. Table 3 summarises these contributions. It can be seen that, despite a significant reduction of the beam current related error, the total uncertainty remains to be dominated by it.

Table 3: Systematic uncertainties, in %, on the value of $\sigma_{\rm vis}$.

Scan Number	I	II-III	IV-V
Bunch charge product	5.6	4.4	3.1
Beam centring	2	2	0.04
Emittance growth & other non-reproducibility	3	3	0.5
Beam-position jitter	—	—	0.3
Length scale calibration	2	2	0.3
Absolute ID length scale	0.3	0.3	0.3
Fit model	1	1	0.2
Transverse correlations	3	2	0.9
Pileup correction	2	2	0.5

The total systematic uncertainty in the October vdM scan is estimated to be 3.4%.

ALGORITHM CONSISTENCY

Fig. 10 gives a comparison of the specific luminosities, as determined during the October vdM scans for all ATLAS luminosity algorithms. The excellent consistency is evident, especially in the plot where all six colliding BCID's are averaged to reduce the statistical scatter.

In the other plots the worse statistics of the offline algorithms is evident. This is no intrinsic deficiency of the algorithms but just a reflection of the smaller number of triggered events available for offline analysis.

LONG-TERM STABILITY

While we have been able to reach a systematic uncertainty well below 5% in the vdM calibration itself, this alone does not assure that we can measure the luminosity with such an accuracy at all times thereafter – or before.

In fact several parameters which can change between ATLAS runs can have an influence on the measured luminosity:

- stability of detector efficiency
- beam-related background
- bunch-spacing (e.g. afterglow level)
- pileup conditions

The first of these points can to a large extent be controlled by frequent calibrations with light pulses – typically once a day for LUCID. The background and afterglow can be estimated from the data and the pileup corrections can be studied by comparing different algorithms.

In all cases, however, it is an asset of ATLAS to have several independent luminosity monitors and algorithms at its disposal. These allow to promptly recognise and diagnose any drifts of individual luminosity algorithms. Such a

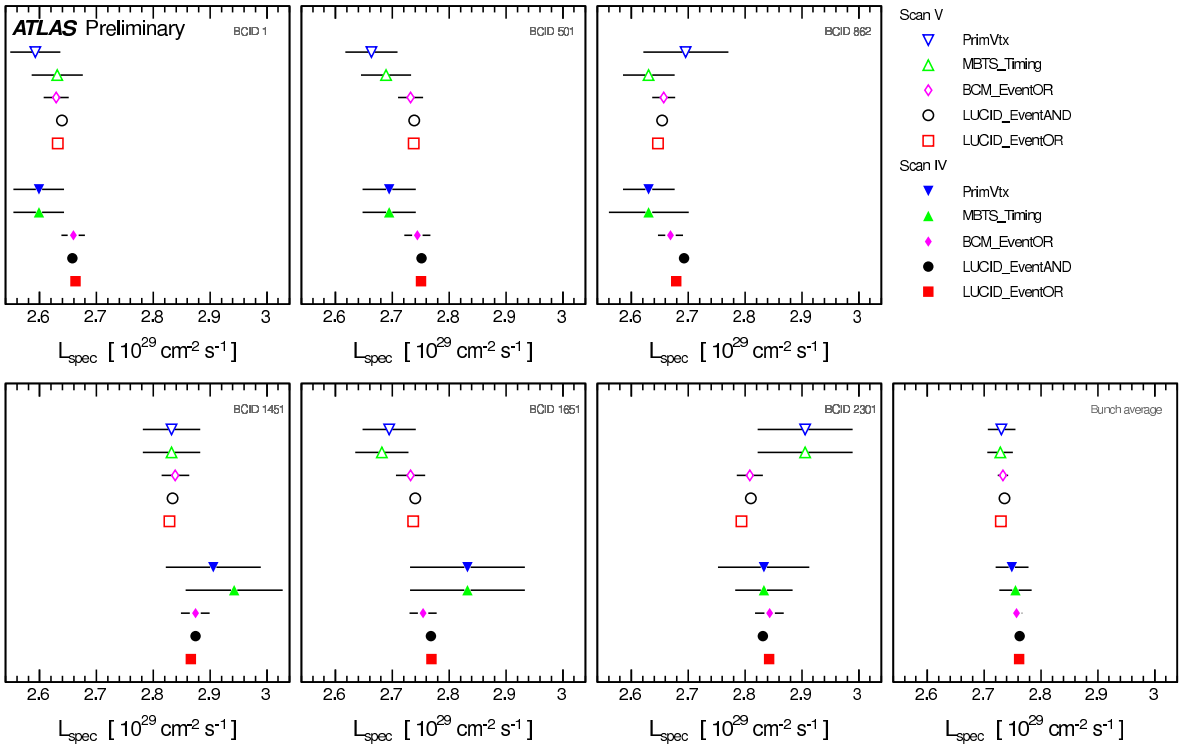

Figure 10: Specific luminosities (Eq. 12 in units of $10^{29}\,\mathrm{cm}^{-2}\mathrm{s}^{-1}$ $(10^{11}$ protons$)^2$ for various ATLAS luminosity detectors and algorithms [6]. The error bars reflect the statistical uncertainties only.

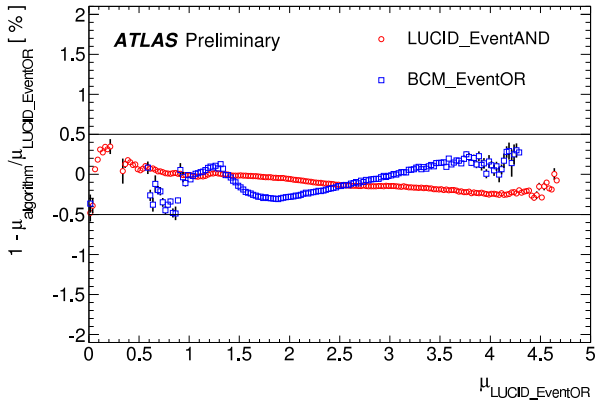

Figure 11: Fractional deviation in average value of μ as obtained using different algorithms with respect to the corresponding value from LUCID-EventOR. The curves are obtained as averages over several runs [6].

constant monitoring ensures that a once established calibration can be maintained stable over long periods of varying beam conditions – although not necessarily over prolonged shutdowns.

In particular, Fig. 11 shows the deviation of the pileup-corrected value of μ for two detectors and algorithms with respect to LUCID-EventOR. All three algorithms are consistent within $\pm 0.5\%$ over the whole range of μ covered by the 2010 LHC run. This indicates that our pileup correction formalism is adequate and also shows that the calibration is stable over time and between runs.

CONCLUSIONS

During the 2010 LHC run the luminosity determination in ATLAS was based on 3 detectors providing online data and additional 4 offline algorithms. This redundancy was very useful for long-term stability monitoring and estimation of detector related systematic effects.

Uncalibrated all of these methods can provide only information about relative luminosity variations. In order to obtain absolute luminosities several van der Meer scans were performed in 2010. These allow to extract the absolute luminosity from beam intensities and detector response as a function of beam separation.

The systematic uncertainties related to the scan procedure have been studied in detail and the final uncertainty in the 2010 luminosity calibration is estimated to be 3.4%. This value does not include stability of the luminosity monitors over time and in varying beam conditions. These effects have to be controlled by intercomparison of the different monitors and algorithms. Such monitoring over the entire 2010 proton-proton operation showed that long-term stability was within $\pm 0.5\%$.

REFERENCES

[1] ATLAS Collaboration, G. Aad et al., *The ATLAS Experiments at the CERN Large Hardon Collider*, JINST **3** (2008) S08003.

[2] ATLAS Collaboration, G. Aad et al., *Luminosity Determination Using the ATLAS Detector*, ATLAS-CONF-2010-060 (2010).

[3] B. Heinemann, these proceedings.

[4] ATLAS Collaboration, G. Aad et al., *Luminosity Determination in pp Collisions at sqrt(s)=7 TeV Using the ATLAS Detector at the LHC*, `arXiv:1101.2185 [hep-ex]` (2011), submitted to EPJC.

[5] S. van der Meer, *Calibration of the effective beam height in the ISR*, CERN-ISR-PO-68-31, (1968).

[6] ATLAS Collaboration, G. Aad et al., *Updated Luminosity Determination in pp Collisions at $\sqrt{s}$=7 TeV using the ATLAS Detector*, ATLAS-CONF-2011-011 (2011).

[7] T. Pauly, these proceedings.